AN EXAMINATION OF THE SUNSPOT AREAL DATASET, 1875–2017: PAPER I, AN OVERVIEW

Robert M. Wilson
NASA Marshall Space Flight Center, NSSTC, Huntsville, Alabama

robert.m.wilson@nasa.gov

ABSTRACT

Examined are annual values of sunspot number (SSN), corrected sunspot area (SSA), number of active region entries (NARE), largest-observed area active region (LAAR), mean area per entry (MAE), highest latitude spot (HLS), and inferred correlations between selected parameters based on the observed data for the years 1875–2017. A number of ±1 standard error of measurement prediction intervals are made regarding the size of the next sunspot cycle (SC) SC25. In particular, based on the even-odd cycle effect, SC25, the next solar cycle, should have maximum annual SSN = 170.4 ± 13.7, maximum annual SSA = 1,730.3 ± 180.0 millionths of a solar hemisphere, and maximum annual NARE = 3,775 ± 510, assuming that it is not a statistical outlier. Also, based on the observed annual minimum value of HLS for 2017 (= 19°), one predicts minimum annual SSN = 7.0 ± 3.2, minimum annual SSA = 41.5 ± 31.7 millionths of a solar hemisphere, minimum annual NARE = 155 ± 76, maximum annual SSN = 136.2 ± 14.8, maximum annual SSA = 1,461.5 ± 261.2 millionths of a solar hemisphere, and maximum annual NARE = 2,771 ± 330 for SC25. As of March 2019, there have been no occurrences of high-latitude new-cycle spots (≥30°) during the decline of ongoing SC24. Monthly values of SSN, SSA, and NARE are now well within the range of expected values indicative of the approaching SC24/25 cycle minimum, especially values since November 2017. Hence, another prolonged cycle-minimum period, as was experienced for SC23/24, may be underway for SC24/25.

INTRODUCTION

Sunspot number (SSN) has been described as being the "longest available record of solar activity," spanning some four centuries in length (Clette et al. 2007). While true, it should be noted that, prior to the use of telescopes, "spots on the Sun" had previously been described by many ancients going back more than 2,000 years, including Theophrastus, Virgil, Abu Alfadhl Giaafar, Averroës of Cordoba, and others (Shove 1950; Hoyt and Shatten 1997; Vaquero et al. 2002; Vaquero 2007; Vaquero and Vázquez 2009; Zito 2016). Even today, "naked-eye sunspots" can occasionally be glimpsed, especially if they are large (cf. Keller and Friedli 1992), and the brighter disk of the Sun is highly attenuated (i.e., through thick clouds, fog, smoke, or when the Sun is close to the horizon).

More recently, sunspot area (SSA) also has come to be used as a general descriptor of the variation of solar activity. In particular, Richard Carrington introduced the technique of photography for measuring SSA at the Royal Observatory in Greenwich, England, in 1874 (Kiepenheuer 1953). Together, images of the Sun taken with photographic plates from Greenwich, England; Cape Town, South Africa; and Kodaikanal, India, have been combined into what is known today as the *Greenwich Photoheliographic Results*, a dataset spanning May 1874 through December 1976 (cf. Yallop and Hohenkerk 1980; Willis et al. 2013). It should be noted that SSA observations are especially important for describing the cyclic and long-term variation of the Sun's

magnetic fields and solar irradiance (cf. Baranyl et al. 2001; Baumann and Solanki 2005; Wilson and Hathaway 2005, 2006; Pevtsov et al. 2013; Hathaway 2015; Wilson 2015).

In an effort to extend the SSA dataset beyond 1976, David Hathaway, a former National Aeronautics and Space Administration (NASA) solar scientist (now retired) utilized solar observations from the Solar Optical Observing Network (SOON) of the United States Air Force (USAF) and the National Oceanic and Atmospheric Administration (NOAA), reformatting them to conform to that of the Royal Greenwich Observatory (RGO) dataset, to provide the necessary data. Together, the combined datasets form the basis for the sunspot areal dataset that extends from May 1874 through the present (see http://solarcyclescience.com/activeregions.html). (Included at the website are comments describing the format of the data and detailing the changes to the data since 1977. It is important to remember that the RGO dataset is one based on photographically determined results, while the USAF/NOAA SOON dataset is one based on visually determined results.)

This paper (Paper I) is anticipated to be the first of at least three papers that will examine the annual variations and inferred correlations that are apparent in the sunspot areal dataset. Paper I provides a general overview of some of the data and examines the inferred relationships to SSN and other parameters, while Paper II will examine annual hemispheric variations, and Paper III will examine annual variations of the magnetic complexity of sunspots.

METHODS AND MATERIALS

Two primary data sources are employed in this study: (1) annual SSN values, available online at http://sidc.oma.be/silso/datafiles, and (2) annual SSA values, available online at http://solarcyclescience.com/activeregions.html. Other parameters taken from the SSA dataset for (a) the RGO interval 1875–1976 and (b) the USAF/NOAA interval 1977–2017 include (1) the yearly total number of active region entries (NARE), (2) the yearly largest-observed active region area and its magnetic classification (LAAR/MC), (3) the yearly mean area per entry (MAE), and (4) the yearly highest latitude sunspot (HLS). Standard statistical analyses are employed in this study and in the presentation of the results. The magnetic classification (MC) of sunspots will be addressed in Paper III.

RESULTS AND DISCUSSION

Figure 1 displays the annual variation of SSN for the interval 1875–2017 (thin line) and the estimated value for 2018 (dashed line) for sunspot cycles (SCs) SC12–SC24. The thick horizontal line is the overall mean, being 82.2 and having a standard deviation *sd* of 64.2 units of SSN. The year marking the division between the RGO and USAF/NOAA datasets is identified (1977), as are the means and *sd*s for the two independent intervals RGO: 1875–1976 and USAF/NOAA: 1977–present. The *t* statistic for the difference in the means for the two independent samples (Lapin 1978) is computed to be $t = -1.1218$, which by hypothesis testing suggests that the difference in means for the two intervals is not statistically significant.

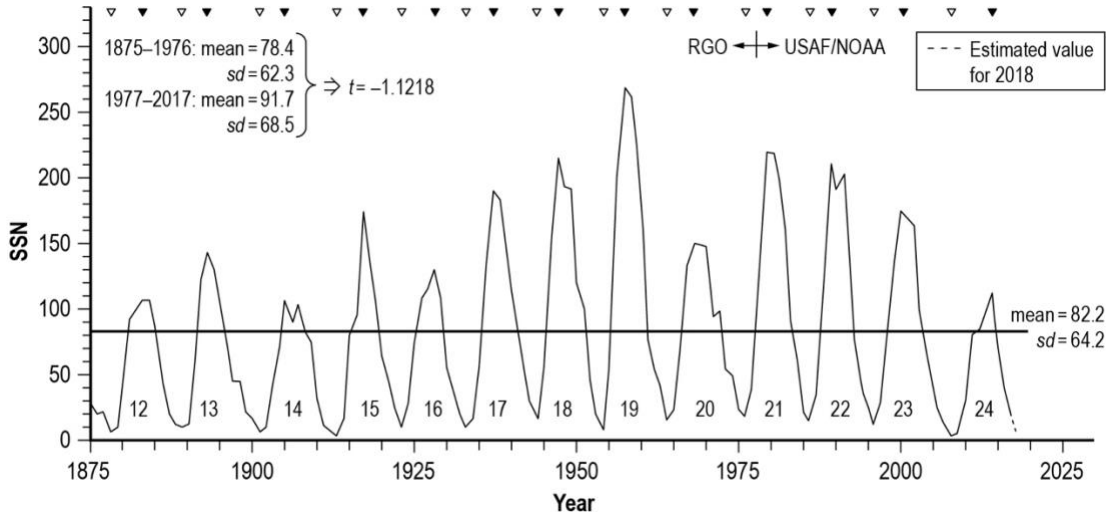

Figure 1. Variation of annual sunspot number (SSN), sunspot cycles (SCs) SC12–SC24. SSN minimum value (min) for each cycle is identified by unfilled triangles, and SSN maximum value (max) for each SC is identified by filled triangles. The interval 1875–1976 represents the Royal Greenwich Observatory (RGO) timeframe, whereas the interval following 1976 represents the United States Air Force/National Oceanic and Atmospheric Administration timeframe. The *t* statistic for independent samples is given.

Notice that each SC has a minimum SSN value (SSN min) and a maximum SSN value (SSN max), denoted by unfilled and filled triangles, respectively. Based on the annual values of SSN, one finds that the rise from SSN min to SSN max has generally been 3–5 years, with only SC24 having a longer rise (6 years). Also, the decline from SSN max to the following SSN min has usually been 7–8 years, with only SC12, SC15, and SC16 having shorter descents (6, 6, and 5 years, respectively). One also observes that the descent is usually 4 years longer than the rise for all SCs except SC12, SC15, and SC16, where these cycles have differences in length as compared to their rise of 1, 2, and 0 years longer, respectively. The duration (or period) of SCs from leading SSN min to following SSN min has always measured 10–12 years. Because SC24 remains ongoing, its descent and SSN min-SSN min duration are yet to be determined, although one strongly suspects that its descent will be ≥6 years, thus yielding SSN min-SSN min duration ≥12 years and inferring SSN min for SC25 to occur in 2020 or later (Wilson 2015, 2017).

SSN max values are observed to have generally increased from SC12 to SC19 and then decreased from SC19 to SC24, with an even-numbered-odd-numbered cycle preferential behavior apparent; i.e., in even-odd-numbered SC pairs, the odd-numbered following SC almost always has been the cycle of larger SSN max, true for five of six known pairs, with only SC23 failing in cycle pair SC22–SC23. In descending order of SSN max, the largest SC is SC19 (269.3), followed by SC21 (220.1), SC18 (214.7), SC22 (211.1), SC17 (190.6), SC23 (173.9), SC15 (173.6), SC20 (150.0), SC13 (142.2), SC16 (129.7), SC24 (113.3), SC12 (106.1), and SC14 (105.5). The mean SSN max measures 168.7 with *sd* = 51.3, and the median SSN max is 173.6. The four largest SCs—SC18, SC19, SC21, and SC22—all have the shortest rise time from SSN min to SSN max (3 years) and were among the shortest in cycle duration (10 years), in addition to all having SSN max >200.

In descending order of SSN min, the cycle with the largest SSN min is SC21 (18.4), followed by SC18 (16.1), SC20 (15.0), SC22 (14.8), SC23 (11.6), SC13 (10.4), SC16 (9.7), SC17 (9.2), SC19 (6.6), SC12 (5.7), SC14 (4.6), SC24 (4.2), and SC15 (2.4). The mean SSN min measures 9.9 with *sd* = 5.1, and the median SSN min is 9.7. For SC24, its SSN measured about 7.0 in 2018 (the 10th year of the ongoing SC), a value well within the range of previously observed SSN min values (2.4–18.4) and consequently indicates that SSN min for SC25 is near.

Figure 2 shows the annual variation of the corrected SSA for the interval 1875–2017 (thin line) and the estimated value for 2018 (dashed line, being about 24.4 millionths of a solar hemisphere) for SC12–SC24. Also shown for comparison are the occurrences of SSN min and SSN max using unfilled and filled triangles as before. As with SSN, the *t* statistic for independent samples is found not to be statistically significant ($t = -1.2227$). Also given is the inferred linear correlation coefficient *r* between SSA and SSN, having $r = 0.972$, inferring that >94% of the variance in SSA can be explained by the variation of SSN (or vice versa). The inferred regression equation is $y = -93.0 + 11.066x$, where *y* is the dependent variable SSA, and *x* is the independent variable SSN. The overall mean SSA is 830.9 millionths of a solar hemisphere, having *sd* = 738.2 millionths of a solar hemisphere. Unlike SSN, which typically appears to be more singularly peaked, SSA often appears to have multiple peaks over the SC (e.g., SC14, SC16, SC18, SC20, SC21, and SC22).

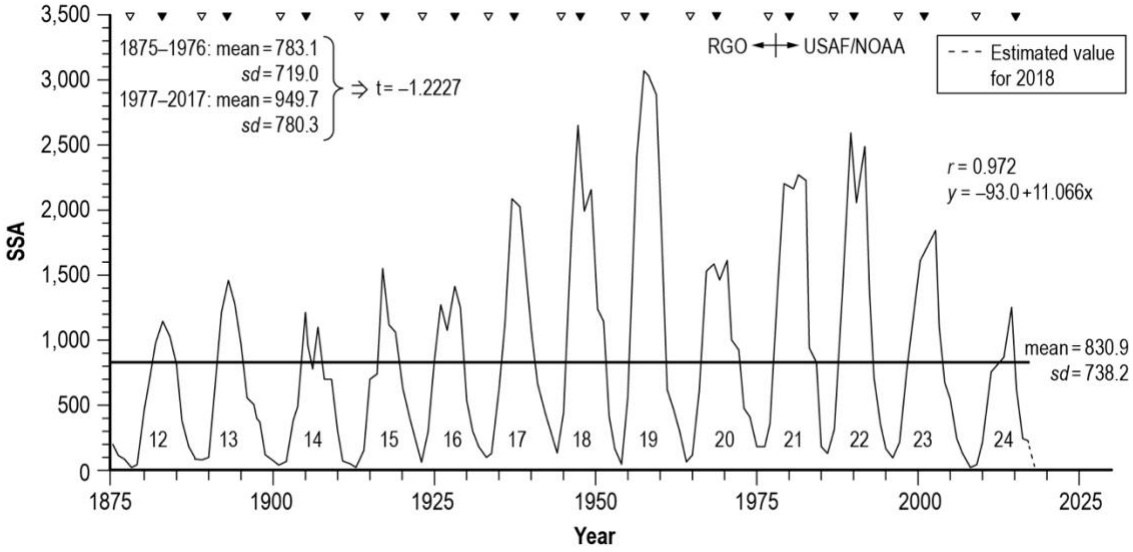

Figure 2. Variation of annual corrected sunspot area (SSA), sunspot cycles (SCs) SC12–SC24. The filled and unfilled triangles have the same meanings as used in Figure 1. The linear correlation coefficient *r* and inferred regression equation for SSA versus sunspot number (SSN) is shown. The *t* statistic for independent samples is given.

As with SSN max values, SSA max values are observed to have generally increased from SC12 to SC19 and decreased from SC19 to SC24—with the odd-numbered SC following the even-odd-numbered cycle pairs, almost always being the cycle of larger SSA max (true for five of six known pairs), with only SC23 failing in cycle pair SC22–SC23. In descending order of SSA max, the largest SC is SC19 (3,048.5), followed by SC18 (2,634.1), SC22 (2,579.2), SC21 (2,270.2),

SC17 (2,072.8), SC23 (1,828.7), SC20 (1,601.3), SC15 (1,533.9), SC13 (1,460.6), SC16 (1,388.9), SC24 (1,252.2), SC14 (1,195.9), and SC12 (1,148.9). The mean SSA max measures 1,847.3 millionths of a solar hemisphere with *sd* = 620 millionths of a solar hemisphere and the median SSA max is 1,601.3 millionths of a solar hemisphere. Close inspection reveals that 10 of 13 SCs have had simultaneous maxima of SSN and SSA, with only SC20, SC21 and SC23 having SSA max lagging SSN max by 2 years.

In descending order of SSA min, the cycle with the largest SSA min is SC21 (166.4), followed by SC18 (124.7), SC22 (124.7), SC17 (91.3), SC23 (81.9), SC13 (76.7), SC16 (54.7), SC20 (53.9), SC19 (34.6), SC14 (27.9), SC24 (22.8), SC12 (22.2), and SC15 (7.5). The mean SSA min measures 68.4 millionths of a solar hemisphere with *sd* = 48.2 millionths of a solar hemisphere and the median SSA min is 54.7 millionths of a solar hemisphere. (As previously noted, the estimated value for SSA in 2018 is 24.4 millionths of a solar hemisphere.)

Figure 3 displays the ratio of SSA to SSN, showing the yearly average SSA per unit SSN. Obviously, the ratio changes significantly over the SC (from about 3.1 to 13.7), usually being greatest near SSN max (e.g., SC12, SC14, SC18, SC22 and SC24) or later during the declining portion of the SC (e.g., SC13, SC15, SC17, SC19, SC21 and SC23). Only SC16 and SC20 had their greatest ratio prior to SSN max. The minimum ratio usually occurs concurrently with SSN min (e.g., SC13, SC15, SC16, SC19, SC20, SC22, and SC24) or just before or after SSN min (e.g., SC14, SC21, and SC23 had their minimum ratio 1 year preceding SSN min, while SC12 and SC18 had their minimum ratio 1 year after SSN min, and SC17 had its minimum ratio 2 years after SSN min). Interestingly, all odd-numbered SCs had their maximum ratio 1–5 years after SSN max, while all even-numbered SCs had their maximum ratio either concurrent with SSN max (e.g., SC12, SC14, SC18, SC22 and SC24) or preceding SSN max by 2 years (e.g., SC16 and SC20). The largest ratio measures 13.67 occurring in 1982 (SC21), which is larger than the 12.56 that occurred in 1959 (SC19, the largest amplitude SC, having SSN max = 269.3 in 1957).

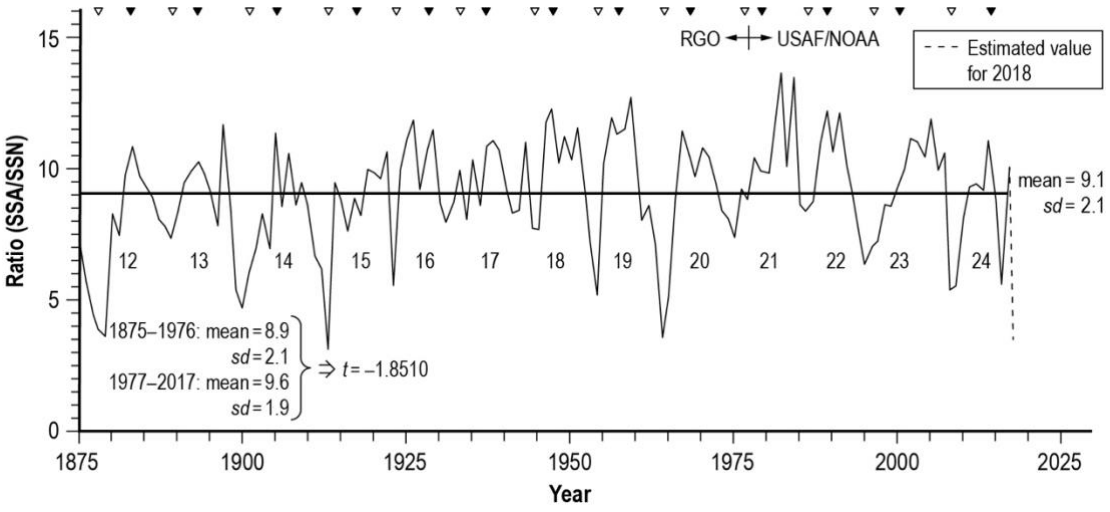

Figure 3. Variation of the annual ratio sunspot area/sunspot number (SSA/SSN), sunspot cycles (SCs) SC12–SC24. The filled and unfilled triangles have the same meanings as used in Figure 1. The *t* statistic for independent samples is given.

Figure 4 shows the annual variation of NARE. Recall that NARE is simply the number of sunspot areal entries per year in the SSA dataset. While NARE has the strongest correlation against SSN (r = 0.982, y = 33.1 + 20.516x), the t statistic for independent samples suggests that a statistically significant difference in the means between the RGO and USAF/NOAA intervals might exist, with the latter interval having more daily entries, on average, than the former. For all cycles, NARE min occurs concurrently with SSN min. For 8 of 12 cycles, NARE max occurs concurrently with SSN max (i.e., SC13, SC15, SC16, SC17, SC18, SC21, SC23 and SC24), while preceding by 1 year for SC20 and following by 1 year for SC12, SC19, and SC22 and by 2 years for SC14. On average, NARE measures about 1,726.0 entries per year (or about 4.7 entries per day) with sd = 1,336.1 entries per year. NARE spans 60 in 1913 (SC15) to 5,439 in 1979 (SC21). SC19, the largest SC in terms of SSN and SSA, had NARE max = 5,016 (1958), yet it was not the largest SC in terms of NARE. This seems to suggest that SC19 was large because it had a larger number of groups (NG) and/or a larger number of individual spots (NS) than SC21. (Recall that, by definition, SSN = 10 NG + NS and that a group is an active region.)

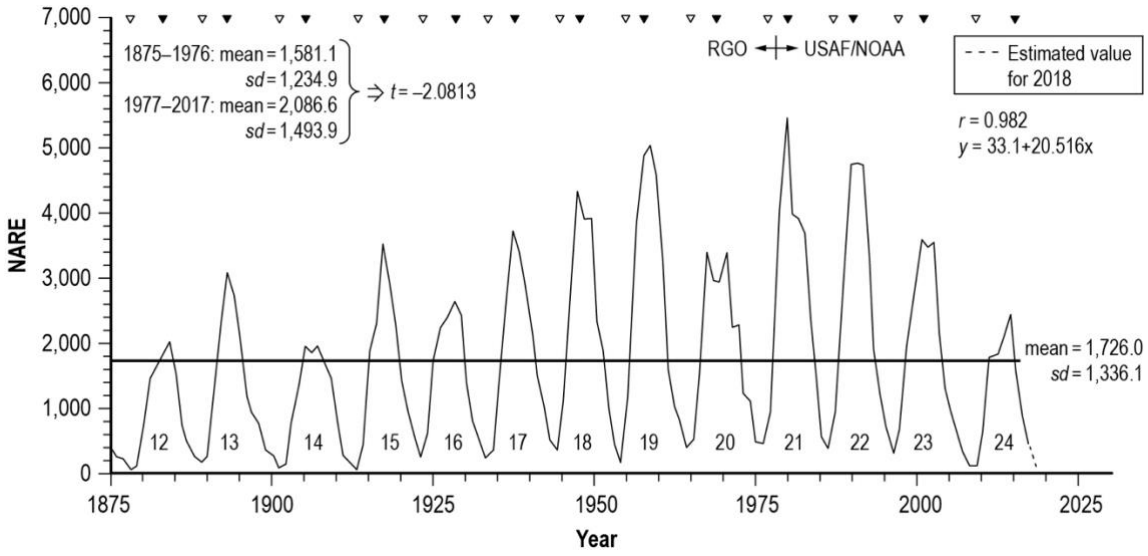

Figure 4. Variation of the annual number of active region entries (NARE), sunspot cycles (SCs) SC12–SC24. The filled and unfilled triangles have the same meanings as used in Figure 1. The linear correlation coefficient *r* and inferred regression equation for NARE versus sunspot number (SSN) is shown. The *t* statistic for independent samples is given.

Regarding NARE max, SC21 has the largest NARE (5,439), followed by SC19 (5,016), SC22 (4,751), SC18 (4,298), SC17 (3,705), SC23 (2,442), SC15 (3,510), SC20 (3,390), SC13 (3,071), SC16 (2,613), SC24 (2,442), SC12 (2,039), and SC14 (1,951). The mean (*sd*) of NARE max is 3,524 (1,115.7), and the median NARE max is 3,510. Regarding NARE min, SC21 has the largest NARE min (426), followed by SC22 (394), SC20 (390), SC18 (370), SC23 (306), SC16 (244), SC17 (225), SC13 (191), SC19 (166), SC24 (122), SC12 (81), SC14 (78), and SC15 (60). The mean (*sd*) of NARE min is 234.8 (131.6), and the median NARE min is 225. The value of NARE for 2018 is 161.

Figure 5 displays the annual variation of LAAR/MC. While LAAR/MC correlates only loosely against SSN, having r = 0.695 and y = 923.7 + 10.792x, it shares a somewhat similar

behavior with SSN, SSA ,and NARE in that there appears to be a general rise from SC12 to about SC18 and a decrease afterwards to SC24 (especially after SC22). The largest sunspot in the interval 1875–2018 occurred in SC18, designated region 1488063. It occurred on April 8, 1947, and measured 6,132 millionths of a solar hemisphere. For SC16, the cycle with the second largest LAAR/MC, region 986103, attained its maximum size on January 19, 1926, and measured 3,716 millionths of a solar hemisphere. For SC19, the largest SC of the modern era in terms of SSN and SSA annual values, its largest active region, designated region 1910900, occurred on January 8, 1959, and measured only 2,805 millionths of a solar hemisphere. Compared to the largest active region of SC18, the largest active region of SC19 is less than half its size.

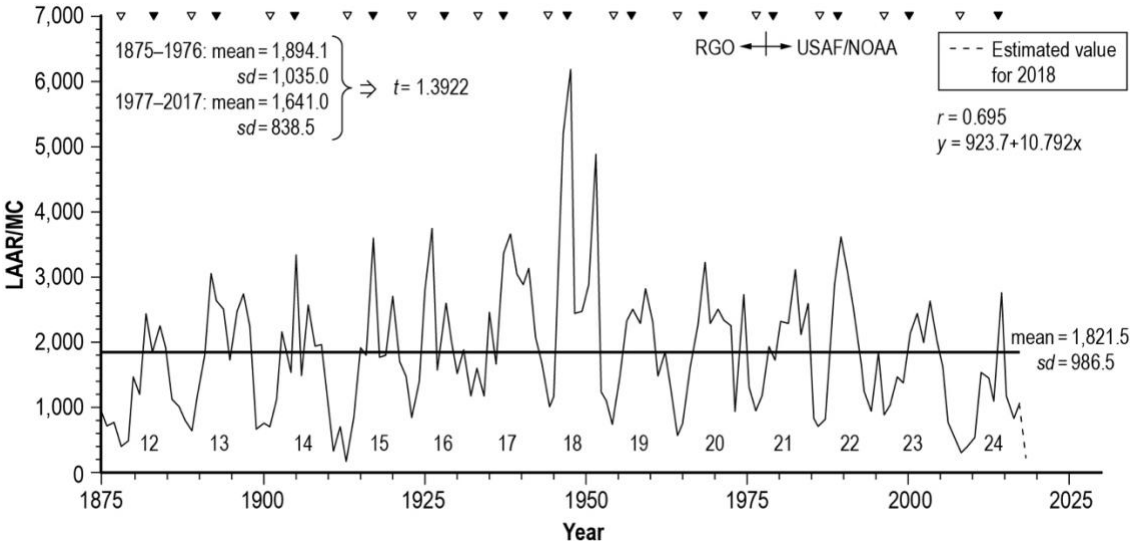

Figure 5. Variation of the annual largest area active region/magnetic class (LAAR/MC), sunspot cycles (SC) SC12–SC24. The filled and unfilled triangles have the same meanings as used in Figure 1. The linear correlation coefficient *r* and inferred regression equation for LAAR/MC versus SSN is shown. The *t* statistic for independent samples is given.

Overall, the mean LAAR/MC measures 1,821.5 millionths of a solar hemisphere (*sd* = 986.5 millionths of a solar hemisphere). Interestingly, SC24's LAAR/MC max is comparable in size to that seen in SC19 (2750 versus 2805). For LAAR/MC max, the progression from largest to smallest SC amplitude values is SC18 (6,132), SC16 (3,716), SC17 (3,627), SC22 (3,600), SC15 (3,590), SC14 (3,339), SC20 (3,202), SC21 (3,100), SC13 (3,038), SC19 (2,805), SC24 (2,750), SC23 (2,610) and SC12 (2,425). The mean LAAR/MC max measures 3,379.5 millionths of a solar hemisphere, with *sd* = 926.5 millionths of a solar hemisphere and a median equal to 3,202 millionths of a solar hemisphere. For 7 of 13 SCs, LAAR/MC max occurs concurrently with SSN max (i.e., SC13, SC14, SC15, SC18, SC20, SC22, and SC24). SC12 and SC16 had their LAAR/MC max 1and 2 years, respectively, prior to SSN max and SC17, SC19, SC21, and SC23 had their LAAR/MC max 1 (SC17), 2 (SC19), and 3 years (SC21 and SC23) following SSN max.

For LAAR/MC min, the progression from largest to smallest value is SC17 (1,155), SC18 (1,010), SC21 (937), SC23 (880), SC16 (831), SC19 (712), SC22 (700), SC13 (639), SC14 (638), SC20 (545), SC12 (402), SC24 (300), and SC15 (138). The mean LAAR/MC min measures 683.6

millionths of a solar hemisphere, with *sd* = 288.9 millionths of solar hemisphere and a median equal to 700 millionths of a solar hemisphere. For 11 of 13 SCs, LAAR/MC min occurs concurrently with SSN min. Only SC14 (2 years) and 17 (1 year) had their LAAR/MC min before SSN min. The value of LAAR/MC for 2018 (SC24) measures 240 millionths of a solar hemisphere.

Figure 6 shows the annual variation of MAE. MAE is simply SSA divided by NARE and then multiplied by the number of days in the year. As with LAAR/MC, there is only a loose correlation between MAE and SSN, having $r = 0.636$ and $y = 124.6 + 0.398x$. The mean MAE measures 157.8 millionths of a solar hemisphere, with *sd* = 40.4 millionths of a solar hemisphere. There is the perception that MAE was declining in value between SC12 and SC15, rising between SC15 and SC19 and declining again after SC19 (through, at least, SC24). Interestingly, MAE max occurred concurrently with SSN max for all even-numbered SCs, while following SSN max by 1–5 years for all odd-numbered cycles. The mean MAE max measures 210.4 millionths of a solar hemisphere, with *sd* = 19.5 millionths of a solar hemisphere and a median equal to 208.6 millionths of a solar hemisphere.

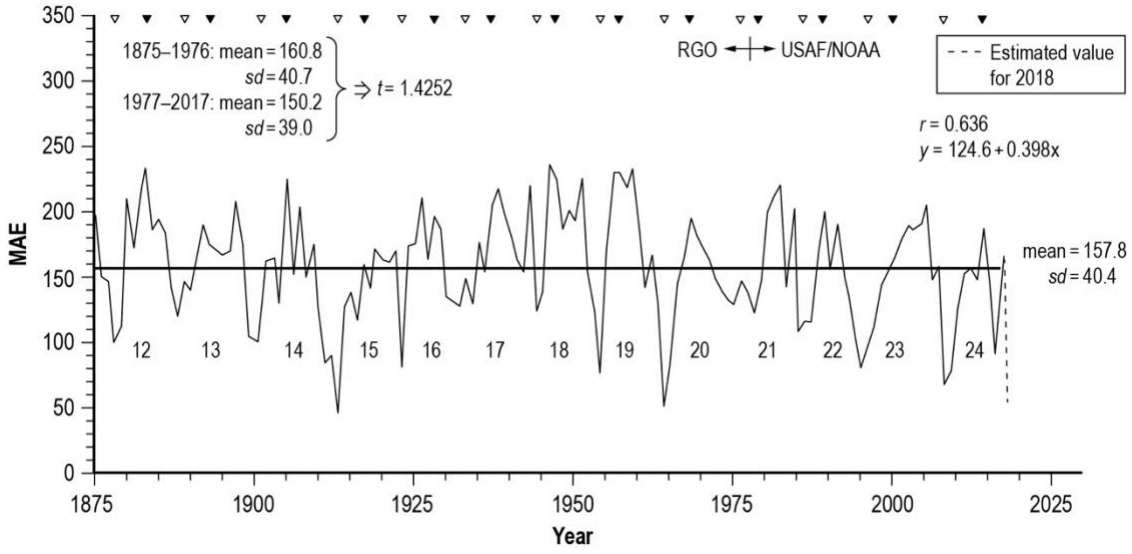

Figure 6. Variation of the annual mean area per entry (MAE), sunspot cycles (SC) SC12–SC24. The filled and unfilled triangles have the same meanings as used in Figure 1. The linear correlation coefficient *r* and inferred regression equation for MAE versus sunspot number (SSN) is shown. The *t* statistic for independent samples is given.

For MAE max, the progression from largest to smallest value is SC18 (234.6), SC12 (234.0), SC19 (232.3), SC14 (225.4), SC21 (219.8), SC17 (218.9), SC16 (208.6), SC13 (206.8), SC23 (203.5), SC22 (198.9), SC20 (193.9), SC24 (187.2), and SC15 (171.2). The mean MAE max measures 210.4 millionths of a solar hemisphere, with *sd* = 19.5 millionths of a solar hemisphere and median equal to 208.6 millionths of a solar hemisphere. For MAE min, the progression from largest to smallest value is SC17 (126.8), SC21 (123.8), SC18 (123.4), SC13 (121.4), SC22 (108.2), SC12 (100.0), SC14 (99.6), SC23 (82.4), SC16 (81.8), SC19 (76.1), SC24 (68.4), SC20 (50.6), and SC15 (45.6). The mean MAE min measures 92.9 millionths of a solar hemisphere, with

sd = 27.9 millionths of a solar hemisphere and a median equal to 99.6 millionths of a solar hemisphere. The value of MAE for 2018 measures 55.3 millionths of a solar hemisphere.

Figure 7 displays the annual variation of HLS. The overall appearance in the variation of HLS is that it was generally rising from SC12 through SC22 and declining afterwards. As with LAAR/MC and MAE, only a loose correlation exists between HLS and SSN ($r = 0.400$ and $y = 30.6 + 0.053x$). The mean HLS measures 34.9°, with *sd* = 8.4°. For HLS max, the progression from largest to smallest value is SC15 (59.5°), SC22 (58.0°), SC19 (50.3°), SC23 (50.0°), SC16 (48.0°), SC20 (46.1°), SC21 (45.6°), SC18 (42.9°), SC17 (42.2°), SC24 (42.0°), SC14 (40.9°), SC13 (40.5°), and SC12 (38.6°). The mean HLS max measures 46.5°, with *sd* = 6.5° and a median equal to 45.6°. For HLS min, the progression from largest to smallest value is SC21 (20.1°), SC16 (29.3°), SC22 (28.0°), SC18 (26.1°), SC17 (25.6°), SC20 (25.2°), SC23 (24.0°), SC15 (21.9°), SC13 and SC19 (20.1°), SC14 (16.4°), SC12 (15.3°) and SC24 (15.0°). The mean HLS min measures 22.8°, with *sd* = 5.2° and a median equal to 24.0°. The value of HLS for 2017 and 2018 measures 19.0° and 32.0°, respectively.

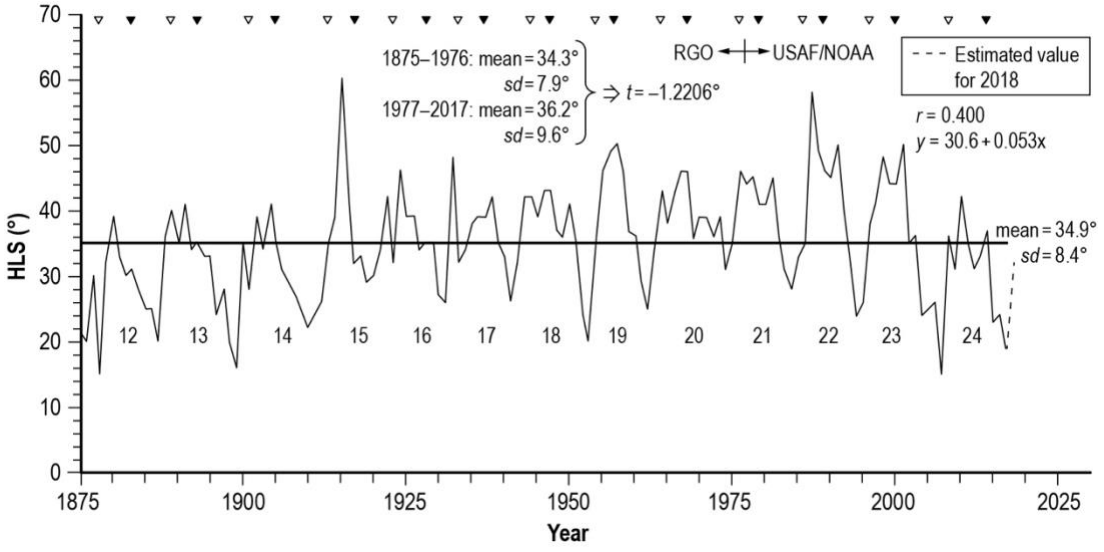

Figure 7. Variation of the annual highest latitude spot (HLS), sunspot cycles (SC) SC12–SC24. The filled and unfilled triangles have the same meanings as used in Figure 1. The linear correlation coefficient *r* and inferred regression equation for annual mean area per entry (MAE) versus SSN is shown. The *t* statistic for independent samples is given.

HLS max is found to almost always occur prior to SSN max. Only SC19 and 23 had HLS max either concurrent with SSN max (SC19) or after SSN max (SC23, +2 years). HLS max occurred 4 years prior to SSN max for SC24, 3 years prior to SSN max for SC12, SC16, and SC21, 2 years prior to SSN max for SC13, SC15, and SC22, and 1 year prior to SSN max for SC14, SC18, and SC20. Similarly, HLS min almost always occurs prior to SSN min. Only SC12 had its HLS min concurrent with SSN min. HLS min occurred 5 years prior to SSN min for SC17, 4 years prior to SSN min for SC16, 3 years prior to SSN min for SC15 and 18, 2 years prior to SSN min for SC13, SC14, SC17, SC20, SC21, SC22, and SC23, and 1 year prior to SSN min for SC19 and SC24. Now in the late stage of SC24, an HLS value indicative of a possible HLS min for SC25

appears to have occurred in 2017 (=19°) since the value for 2018 (=32°) is higher. Near SSN min, there is a change from lower latitude old cycle spots to higher latitude new cycle spots, where new cycle spots are differentiated from old cycle spots by means of their leading and following magnetic polarity. For even-numbered SCs, the northern hemisphere of the Sun has negative-leading and positive-following magnetic polarity (reversed in the southern hemisphere). For odd-numbered SCs, the leading and following hemispheric polarities are reversed. The overlap in old and new cycles about SSN min is about 1–3 years (Howard 1977).

Figure 8 illustrates the even-odd cycle effect for SSN max, SSA max, and NARE max. Given are the linear correlation coefficients and inferred regression equations, ignoring SC22/23. Located along the *x*-axis are arrows signifying the max values from SC24. For SSN max, the observed value of SSN max for SC24 (= 113.3) suggests that SSN max for SC25, the next SC, is expected to be about 170.4 ± 13.7, presuming that cycle pair SC24/25 will not be a statistical outlier (as SC22/23). For SSA max and NARE max, predicted values for SC25 are 1,730.3 ±180.0 millionths of a solar hemisphere and 3,775 ± 510 entries.

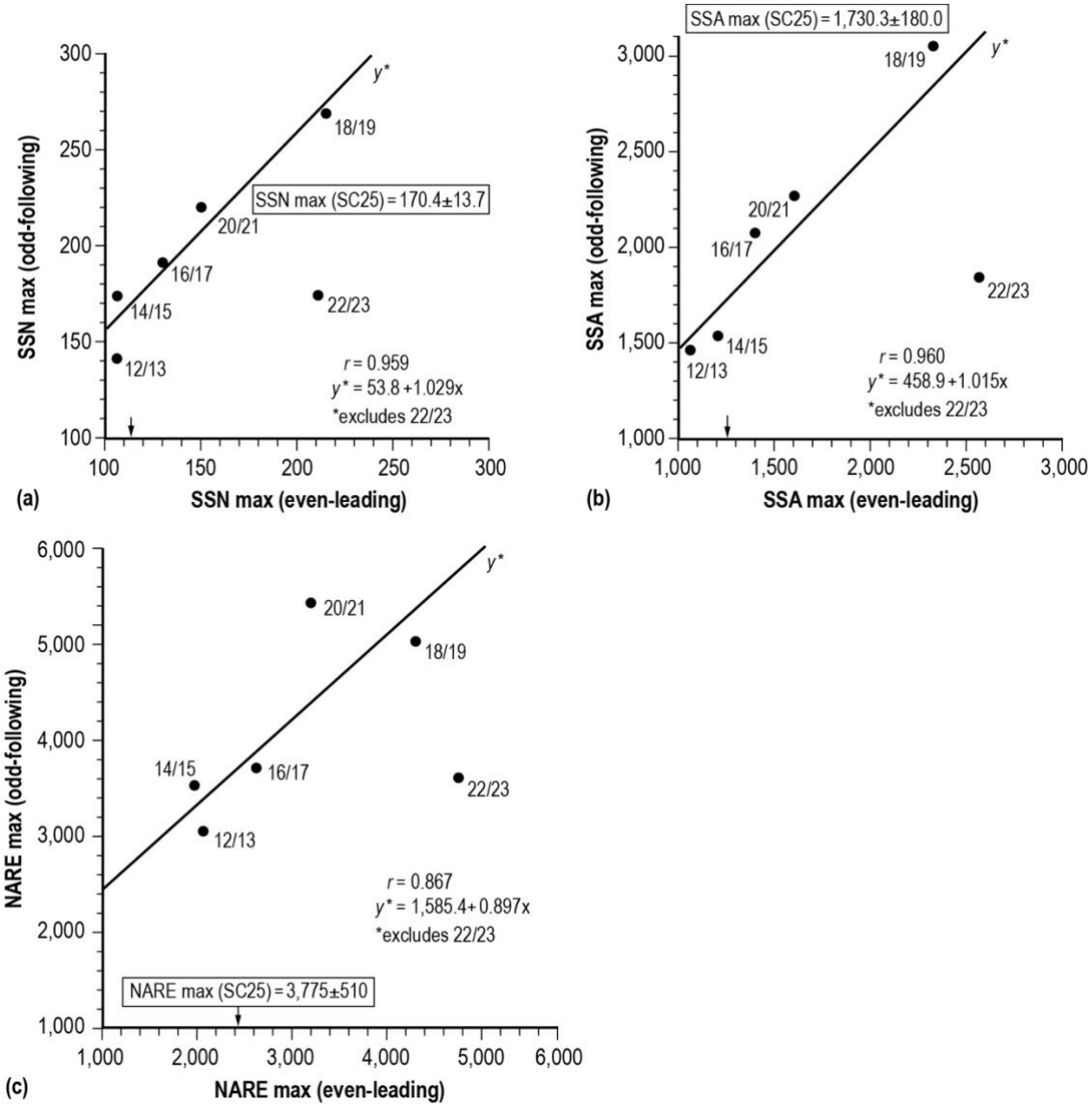

Figure 8. Scatterplots of (a) maximum sunspot number value (SSN max) (odd-following) versus SSN max (even-leading), (b) maximum sunspot area value (SSA max) (odd-following) versus SSA max (even-leading) and (c) maximum number of active region entries value (NARE max) (odd-following) versus maximum number of active region entries value (NARE max) (even-leading) for even-odd sunspot cycle pairs SC12/13–SC22/23. The linear correlation coefficient *r* and inferred regression equation is given, based on the exclusion of cycle pair SC22/23, which is a statistical outlier. The arrow along the x-axis of each scatterplot represents the max value for SC24. Based on the inferred regression and the SC24 parametric value, the ±1 standard error of measurement prediction interval for each parameter is given for the next SC, SC25.

Figure 9 shows the scatterplots and inferred relationships between SSN min, SSN max, SSA min, SSA max, NARE min, and NARE max against the HLS min values. HLS min is an intriguing parameter in that it generally occurs several years in advance of min values of SSN, SSA, and NARE and might be of predictive value for both the following min and max values of the parameters. For SSN min versus HLS min, $r = 0.772$ and $y = -7.3 + 0.75x$, inferring that SSN min for SC25 is expected to measure about 7.0 ± 3.2 (i.e., the ±1 standard error of estimate prediction interval), using HLS min = 19°, the observed value for 2017, indicated by the downward pointing arrow along the *x*-axis. Based on Fisher's exact test for 2×2 contingency tables (determined using the parametric medians, shown as the thin vertical and horizontal lines), the probability *P* of obtaining the observed result, or one more suggestive of a departure from independence (chance), is $P = 2.0\%$. In each of the charts, the numbers beside the filled circles refer to the solar cycle number. In particular, five of six solar cycles having HLS min <24° are expected to have SSN min <9.7, while six of seven solar cycles having HLS min ≥24° are expected to have SSN min ≥9.7. SSN is known to measure 7.0 in 2018, with a lower value expected for 2019. Hence, SC24 appears to now be experiencing an extended solar minimum, one which may last at least through 2019 and probably through 2020.

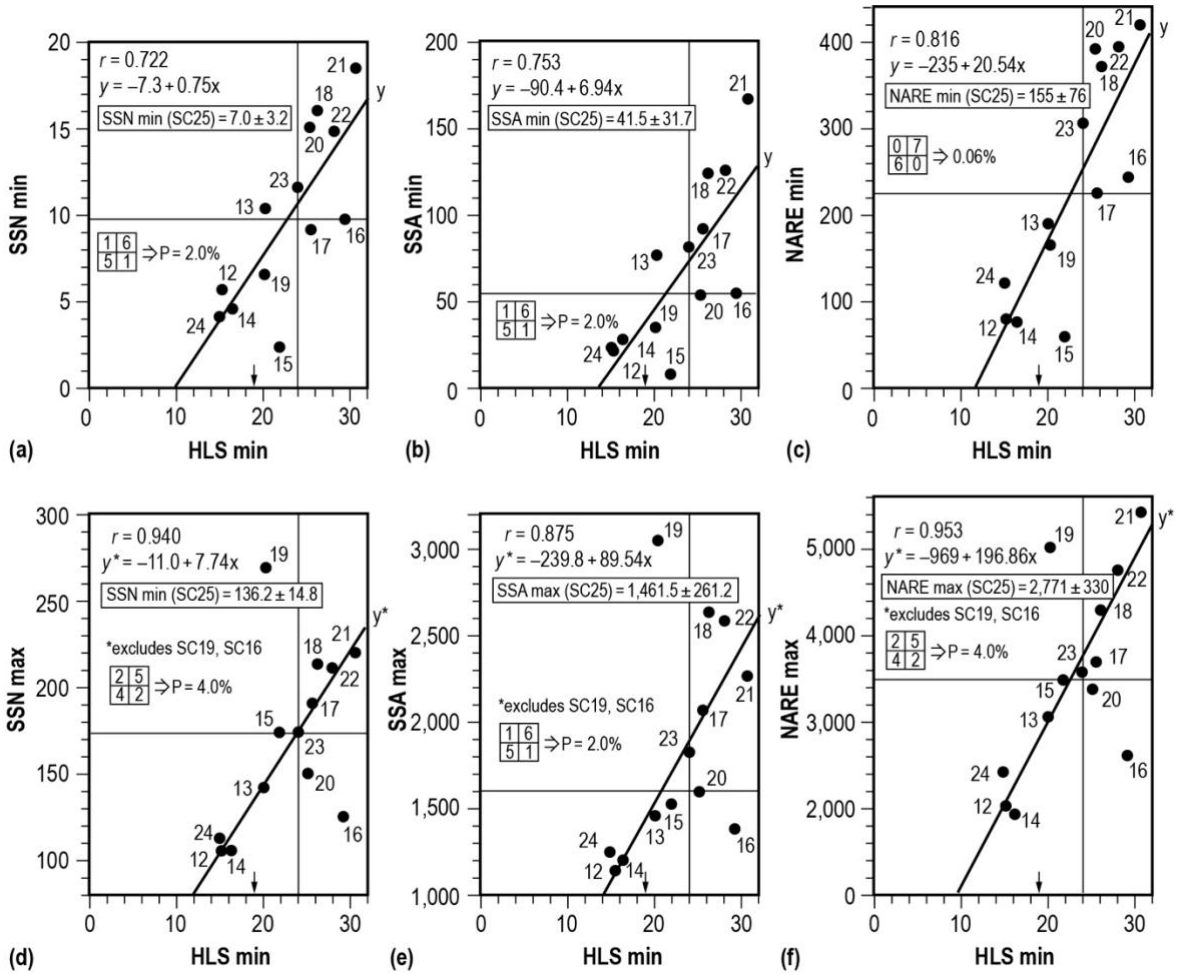

Figure 9. Scatterplots of (a) minimum sunspot number value (SSN min) versus the highest latitude spot minimum value (HLS min), (b) minimum sunspot area value (SSA min) versus highest latitude spot minimum value (HLS min), (c) NARE min versus HLS min, (d) maximum sunspot number value (SSN max) versus HLS min, (e) SSA max versus HLS min and (f) NARE max versus HLS min for SC12–SC24. HLS min is the smallest annual HLS value occurring either prior to or concurrent with the occurrence of SSN min. Shown are the linear correlation coefficients *r* and the inferred regression equation in each scatterplot, the probability *P* of obtaining the observed result, or one more suggestive of a departure from independence (chance), based on the 2×2 contingency tables (determined by the median values, the thin vertical and horizontal lines) and the estimated parametric values for SC25, the next SC. The arrow along the x-axis is the 2017 observed value of HLS (= 19°). For SSN max, SSA max, and NARE max, SC16 and SC19 have been excluded, since they appear to be statistical outliers.

For SSA versus HLS min and NARE min versus HLS min, $r = 0.753$ and 0.816 and $P =$ 2.0% and 0.06%, respectively. Based on the inferred linear regressions, SSA min and NARE min for SC25 are expected to measure about 41.5 ± 31.7 millionths of a solar hemisphere and 155 ± 76, respectively.

For SSN max, SSA max and NARE max versus HLS min—ignoring the values for SC16 and SC19 (statistical outliers)—strong linear correlations are inferred to exist ($r = 0.940$, $r = 0.875$, and $r = 0.953$, respectively). Using HLS = 19°, one expects SC25 to have SSN max = 136.2 ± 14.8, SSA max = 1,461.5 ± 261.2, and NARE max = 2,771 ± 330, assuming SC25 is not a statistical outlier.

Figure 10 displays the observed monthly spot latitudes (ignoring hemispheric notation), monthly number of spotless days (NSD), monthly SSN, monthly SSA and monthly NARE for the interval January 2016 through the end of 2018. As yet, there has been no occurrence of a high-latitude (≥30°) new cycle spot, which would be indicative of the approaching SC25 minimum. A new cycle spot was observed in August 2018, but it was located at low latitude (region 12720, 8° North). The spot (12699) located at 32° in January 2018 was a magnetically simple spot (i.e., a unipolar spot group). Near cycle minimum, new cycle spots at higher latitude become greater in number, while old cycle spots at lower latitudes become fewer in number, with the overlap of new and old cycles being about 1–3 years (Howard 1977).

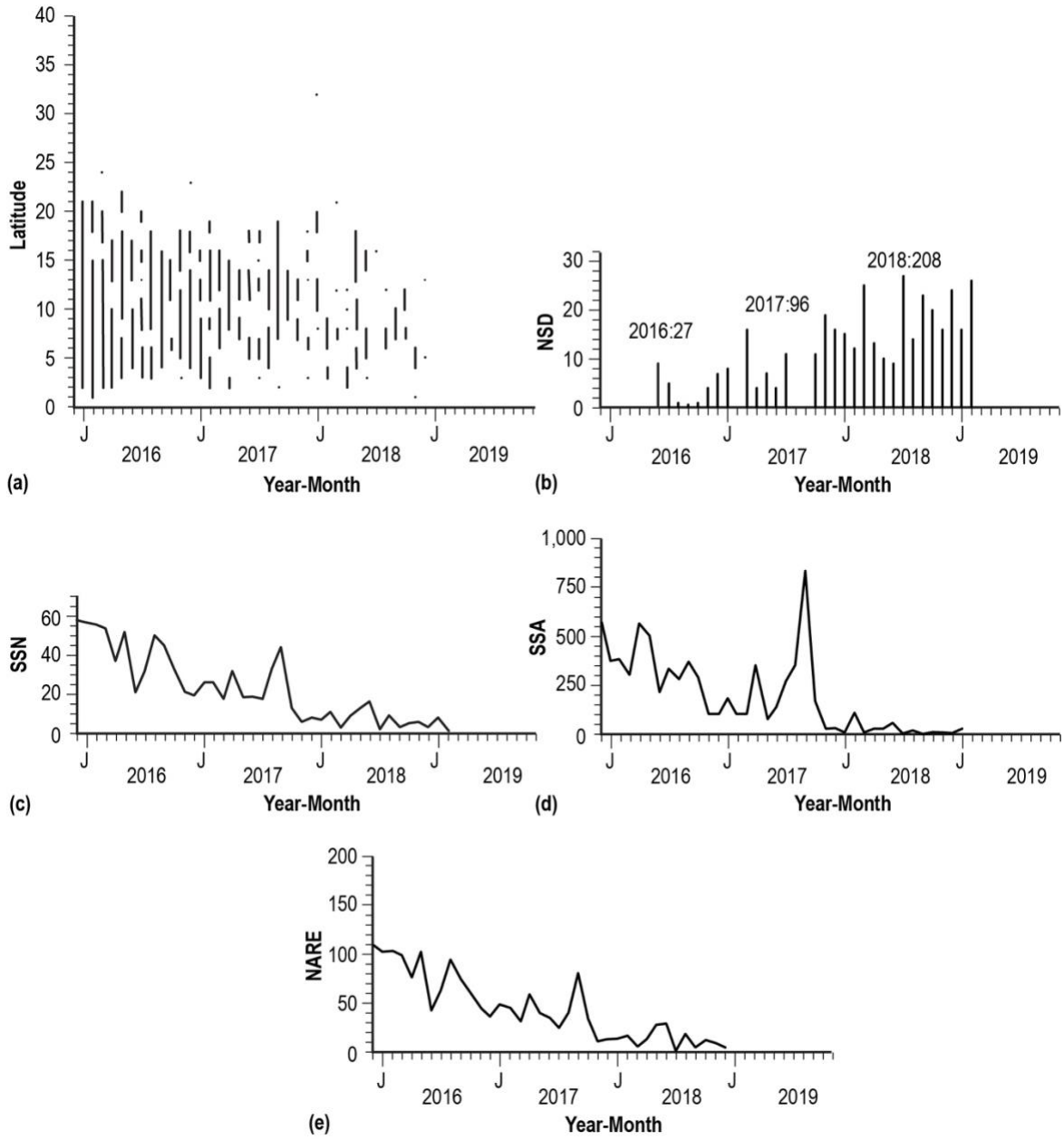

Figure 10. Plots of observed monthly values of (a) spot latitudes (ignoring hemispheric location), (b) number of spotless days (NSD), (c) sunspot number (SSN), (d) sunspot area (SSA) and (e) number of active region entries (NARE) for 2016–2018. Monthly values of SSN, SSA and NARE since late 2017 are indicative of sunspot minimum conditions. As yet, there has been no occurrence of new cycle high-latitude spots, which generally occurs near SC minimum. Old and new cycle spots typically overlap about 1–3 years.

In terms of NSD, there were 208 spotless days in 2018. In January and February 2019, there were 15 and 27 spotless days, respectively. SC15 had the greatest NSD (311) at SSN min (1913), followed by SC14 (287 in 1901), SC12 (280 in 1878), SC24 (265 in 2008), SC10 (261 in 1856), SC19 (241 in 1954), SC17 (240 in 1933), SC11 (222 in 1867), SC13 (212 in 1889) and SC16 (200 in 1923). SC18, SC20, SC21, SC22 and SC23 all had NSD <200 (Wilson 2017). NSDs have been increasing, with 10 months in 2018 having NSD ≥10 days per month and 4 months having NSD ≥20 days per month. Associated with this is a sharp reduction in monthly mean SSN, SSA and NARE. Late 2017 appears to mark the beginning of an extended period of solar minimum, one that could persist for 1–3 years or more.

In conclusion, this study (Paper I) has examined the variation of the annual means of SSN, SSA, NARE, LAAR/MC, MAE, and HLS for the years 1875–2017 and inferred correlations between selected parameters. Regarding SSN, one finds that the descent duration of all SCs SC12–SC23 has always been equal to or longer than their ascent duration, inferring that the present SC24 (ascent duration = 6 years) will have a descent duration ≥6 years and a SSN min-SSN min duration (i.e., ascent + descent duration) ≥12 years, suggesting that SSN min occurrence for SC25 will be the year 2020 or later. Generally, SSA and NARE closely mimic SSN, having $r \geq 0.97$, although SSA max is found to have followed SSN max by 2 years in SC20, SC21, and SC23. Interestingly, all odd-numbered SCs had their maximum ratio of SSA/SSN 1–5 years after SSN max, while all even-numbered SCs had their maximum ratio of SSA/SSN either concurrent with or preceding SSN max by 2 years. The largest SSA/SSN ratio (=13.67) occurred in 1982 (SC21). The largest NARE occurred in 1979 (=5,439, SC21). The largest individual spot group occurred on April 8, 1947 (SC18), measuring 6,132 millionths of a solar hemisphere. Interestingly, the largest spot groups occurring in SC19 (the largest SC in terms of SSN and SSA) and SC24 (the third smallest cycle in terms of SSN and SSA) are of comparable size (2,805 and 2,750 millionths of a solar hemisphere, respectively). Inferred correlations for LAAR/MC, MAE and HLS against SSN are not particularly strong, having $r < 0.7$. Interestingly, one finds that MAE max is observed to have occurred concurrently with SSN max for all even-numbered cycles, while following SSN max by 1–5 years for all odd-numbered cycles. Also, interestingly, HLS min is found to have almost always occurred prior to SSN min, with only SC12 having had concurrent occurrences of HLS min and SSN min. It appears that HLS min for SC25 may have occurred in 2017, measuring 19°. Based on the inferred strong correlations between minimum and maximum values of SSN, SSA, and NARE against HLS min, one predicts SC25, the next SC, to have the following ±1 standard error prediction intervals: SSN min = 7.0 ± 3.2, SSA min = 41.5 ± 31.7 millionths of a solar hemisphere, NARE min = 155 ± 76, SSN max = 136.2 ± 14.8, SSA max = 1,461.5 ± 261.2 millionths of a solar hemisphere, and NARE max = 2,771 ± 330. Based on the inferred even-odd cycle preferential behavior, assuming SC25 is not a statistical outlier, one predicts SSN max = 170.4 ± 13.7, SSA max = 1,730.3 ± 180.0 millionths of a solar hemisphere and NARE max = 3,775 ± 510 for SC25. SC24/25 appears to have begun an extended cycle minimum beginning about November 2017. As yet, there have been no observed high-latitude (≥30°) new-cycle spots, something which generally heralds the impending onset of the new solar cycle.

LITERATURE CITED

Baranyi, T., L. Gyori, A. Ludmány, and H.E. Coffey 2001. Comparison of sunspot area data bases, *Mon. Not. R. Astron. Soc.*, 323, pp. 223–230.

Baumann, I. and S. K. Solanki 2005. On the Size Distribution of Sunspot Groups in the Greenwich Sunspot Record 1874–1976, *Astron. Astrophys.*, 443(3), pp. 1061–1066.

Clette, F., D. Berghmans, P. Vanlommel, R. A. M. Van der Linden, A. Koeckelenbergh, and L. Wauters 2007. From the Wolf number to the International Sunspot Index: 25 years of SIDC, *Adv. Space Res.*, 40, pp. 919–928.

Hathaway, D. H. 2015. The Solar Cycle, *Living Reviews in Solar Physics*, 12(4), 81 pp.

Howard, R. 1977. Chapter 2. Solar Cycle, Solar Rotation and Large-Scale Circulation, in *Illustrated Glossary for Solar and Solar-Terrestrial Physics*, A. Bruzek and C. J. Durrant (eds.), D. Reidel Publishing Co., Dordretch, Holland, pp. 7–12.

Hoyt, D. V. and K. H. Schatten 1997. *The Role of the Sun in Climate Change*, Oxford University Press, New York, NY, 279 pp.

Keller, H. U. and T. K. Friedli 1992. Visibility Limit of Naked-Eye Sunspots, *Q. J. Roy. Astron. Soc. Journal Royal Astronomical Society*, 33, pp. 83–89.

Kiepenheuer, K. O. 1953. Chapter 6. Solar Activity, *The Sun*, G. P. Kuiper (ed.), *The Solar System*, I, The Univ. Chicago Press, Chicago, IL, pp. 322–465.

Lapin, L. 1978. *Statistics for Modern Business Decisions*, 2nd ed., Harcourt Brace Jovanovich, Inc., New York, NY pp. 486–487.

Pevtsov, A. A., L. Bertello, A. G. Tlatov, A. Kilcik, Y. A. Nagovitsyn and E. W. Cliver 2013. Cyclic and Long-Term Variation of Sunspot Magnetic Fields, in González Hernández, I. R. Komm, A. Pevtsov and J. Leibacher (eds.), *Solar Origins of Space Weather and Space Climate*, Springer, New York, New York, pp. 157–166.

Schove, D. J. 1950. The Earliest Dated Sunspot, *Journal British Astronomical Association*, 61, pp. 22–25.

Vaquero, J. M., M. C. Gallego and J. A. García 2002. A 250-year cycle in naked-eye observations of sunspots, *Geophysical Research Letters*, 29, pp.1997–2000.

Vaquero, J. M. 2007. Historical Sunspot Observations: A Review, *Advances in Space Research*, 40, pp. 929–941.

Vaquero, J. M. and M. Vázquez 2009. Chapter 2. Naked-Eye Sunspots, *The Sun Recorded Through History*, Astrophysics and Space Science Library 361, pp. 57–102.

Willis, D. M., H. E. Coffey, R. Henwood, E. H. Erwin, D. V. Hoyt, M. N. Wild and W. F. Denig 2013. The Greenwich Photo-heliographic Results (1874 – 1976): Summary of the Observations, Applications, Datasets, Definitions and Errors. *Solar Physics*, 288(1), pp. 117–139.

Wilson, R. M. 2015. Sunspot Cycle Characteristics based on the Newly Revised Sunspot Number, *Journal of the Alabama Academy of Science*, 86, pp. 203–221.

Wilson, R. M. 2017. Number of Spotless Days in Relation to the Timing and Size of Sunspot Cycle Minimum, *Journal of the Alabama Academy of Science*, 88, pp. 96–120.

Wilson, R. M. and D. H. Hathaway 2005. A Comparison of Rome Observatory Sunspot Area and Sunspot Number Determinations with International Measures, 1958–1998, NASA/TP—2005–214191, NASA Marshall Space Flight Center, Huntsville, Alabama, 24 pp.

Wilson, R. M. and D. H. Hathaway 2006. On the Relation between Sunspot Area and Sunspot Number, NASA/TP—2006–214324, NASA Marshall Space Flight Center, Huntsville, Alabama, 24 pp.

Yallop, B. D. and C. Y. Hohenkerk 1980. Distribution of sunspots 1874–1976, *Sol. Phys.*, 68(2), pp. 303–305.

Zito, R. 2016. Possible Mesoamerican Naked-eye Observation of Sunspots – V: Evidence from Río Azul Tomb I Murals and Related Artifacts, *Sociology and Anthropology*, 4(11), pp. 953–965, doi:10.13189/sa.2016.041102.